JOURNAL OF AGRICULTURAL AND FOOD CHEMISTRY

Highly Acylated (Acetylated and/or *p*-Coumaroylated) Native Lignins from Diverse Herbaceous Plants

José C. del Río,*,† Jorge Rencoret,† Gisela Marques,† Ana Gutiérrez,† David Ibarra,‡ J. Ignacio Santos,‡ Jesús Jiménez-Barbero,‡ Liming Zhang,§ and Ángel T. Martínez‡

Instituto de Recursos Naturales y Agrobiología de Sevilla, CSIC, P.O. Box 1052, 41080 Seville, Spain; Centro de Investigaciones Biológicas, CSIC, Ramiro de Maeztu 9, E-28040 Madrid, Spain; and Fiber and Polymer Technology, Royal Institute of Technology (KTH), SE-100 44 Stockholm, Sweden

The structure of lignins isolated from the herbaceous plants sisal (*Agave sisalana*), kenaf (*Hibiscus cannabinus*), abaca (*Musa textilis*) and curaua (*Ananas erectifolius*) has been studied upon spectroscopic (2D-NMR) and chemical degradative (derivatization followed by reductive cleavage) methods. The analyses demonstrate that the structure of the lignins from these plants is highly remarkable, being extensively acylated at the γ-carbon of the lignin side chain (up to 80% acylation) with acetate and/or *p*-coumarate groups and preferentially over syringyl units. Whereas the lignins from sisal and kenaf are γ-acylated exclusively with acetate groups, the lignins from abaca and curaua are esterified with acetate and *p*-coumarate groups. The structures of all these highly acylated lignins are characterized by a very high syringyl/guaiacyl ratio, a large predominance of β-*O*-4′ linkages (up to 94% of all linkages), and a strikingly low proportion of traditional β-β′ linkages, which indeed are completely absent in the lignins from abaca and curaua. The occurrence of β-β′ homocoupling and cross-coupling products of sinapyl acetate in the lignins from sisal and kenaf indicates that sinapyl alcohol is acetylated at the monomer stage and that, therefore, sinapyl acetate should be considered as a real monolignol involved in the lignification reactions.

KEYWORDS: Lignin; herbaceous plants; sinapyl acetate; sinapyl *p*-coumarate; 2D-NMR; HSQC; DFRC; sisal; kenaf; abaca; curaua

INTRODUCTION

Lignins are complex natural biomacromolecules characteristic of vascular plants, where they provide mechanical support. In addition, lignin waterproofs the cell wall, enabling transport of water and solutes through the vascular system, and plays a role in protecting plants against pathogens (*1*). The lignin polymer results from the random oxidative coupling of *p*-hydroxycinnamyl monolignols mediated by laccases and/or peroxidases (*2, 3*). The three primary monolignols are *p*-coumaryl, coniferyl, and sinapyl alcohols, which produce, respectively, *p*-hydroxyphenyl (H), guaiacyl (G), and syringyl (S) phenylpropanoid units when incorporated into the lignin polymer.

However, it is now widely accepted that other monomers also participate in coupling reactions giving rise to the lignin macromolecule. This is the case of γ-acylated (with acetate, *p*-hydroxybenzoate and/or *p*-coumarate groups) lignins, which have been discovered in many plants. Different grass lignins are partially *p*-coumaroylated, and some hardwood lignins such as poplar, aspen, or willow lignins are *p*-hydroxybenzoylated (*3*−*11*). Acetylated lignin units have also been reported to occur in many plants (*12*−*16*). Characteristic products from sinapyl and coniferyl acetate coupling have been detected upon degradative techniques (Py-GC/MS and derivatization followed by reductive cleavage, DFRC) in the lignin of several plants characterized by having a high S/G ratio such as sisal, kenaf, abaca, and jute (*15, 16*). Previous studies have shown that lignin from these plants is acetylated exclusively at the γ-position of the side chain and that this acetylation occurred predominantly on S units (*12*−*16*). Moreover, these studies have provided strong evidence that sinapyl acetate is implicated as a monomer in lignification in several plants and that the naturally acetylated lignin derives not from acetylation of the lignin polymer but from polymerization of preacetylated monolignols (*14, 16, 17*). The same seems also to occur with sinapyl *p*-coumarate and sinapyl *p*-hydroxybenzoate (*17*−*19*).

We have recently shown, using a previously developed modification of the DFRC method to allow detection of natural acetate groups (*13*) (the so-called DFCR′ methodology) that lignin γ-acetylation is widespread, and probably ubiquitous,

* Author to whom correspondence should be addressed (e-mail delrio@irnase.csic.es; telephone +34 95 462 4711; fax +34 95 462 4002).
† Instituto de Recursos Naturales y Agrobiología de Sevilla, CSIC.
‡ Centro de Investigaciones Biológicas, CSIC.
§ Royal Institute of Technology (KTH).

10.1021/jf800806h CCC: $40.75
Published on Web 09/30/2008

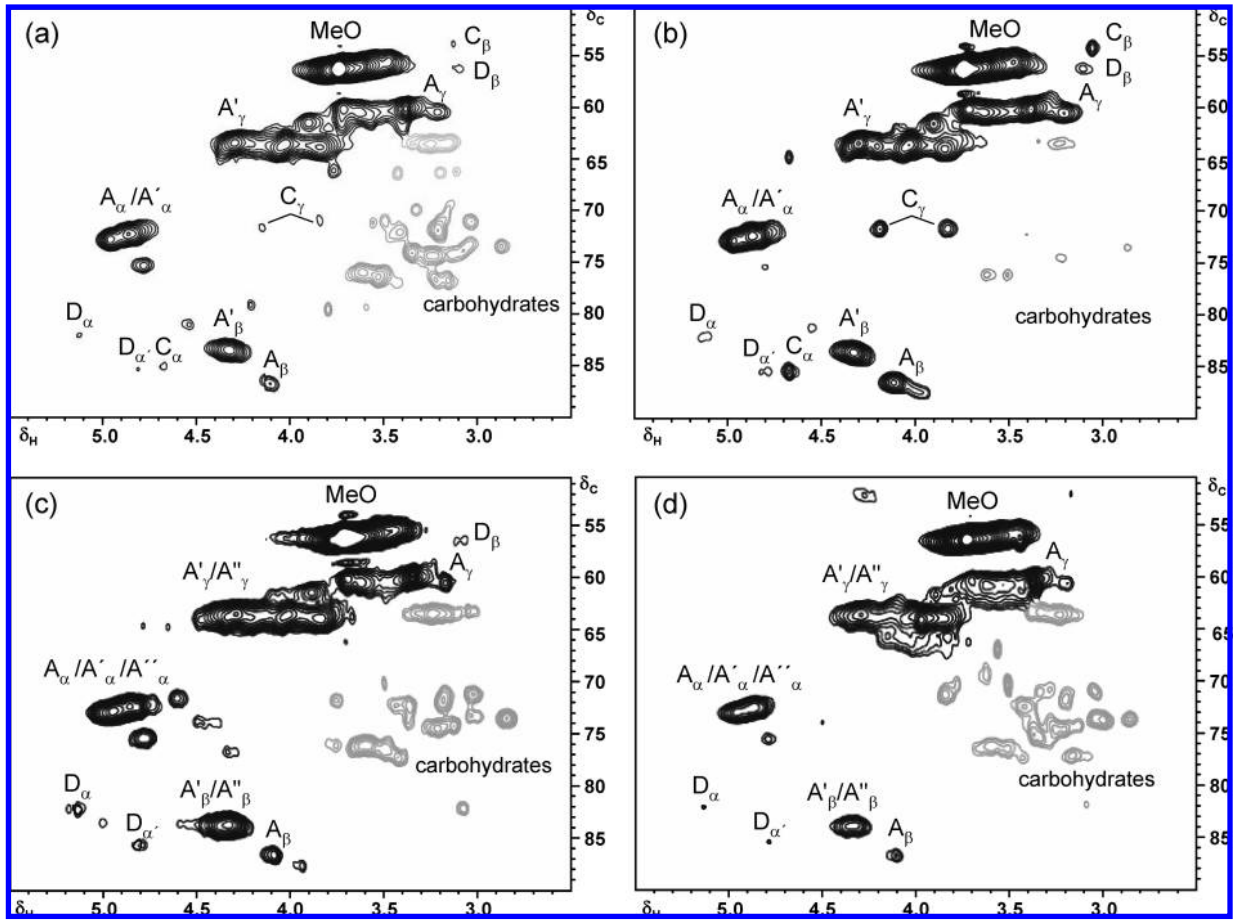

Figure 1. Expanded side-chain region, δ_C/δ_H 50−90/2.5−5.5, of the HSQC spectra of the lignins from (**a**) sisal, (**b**) kenaf, (**c**) abaca, and (**d**) curaua. Carbohydrate signals are presented in gray. See **Table 1** for signal assignment and **Figure 3** for the main lignin structures (A−D) identified.

among angiosperms, although to different extents, but is absent from conifers (*16*). Moreover, the lignins of many plants (e.g., the nonwoody sisal, kenaf, abaca, or the hardwood hornbeam) are particularly extensively acetylated (up to 80% of the S-lignin moieties) (*16*). However, the DFRC degradation method cleaves only α- and *β*-aryl ether bonds, allowing only the analysis of the monomeric degradation products released from noncondensed etherified lignin units. Therefore, the DFRC method, although extremely useful, does not give information of the whole macromolecule, and the extent of lignin acylation may be actually different from that estimated.

Spectroscopic techniques, and particularly 1D- and 2D-NMR, can provide information of the structure of the whole macromolecule and are powerful tools for lignin structural elucidation (*7, 20*−*24*). Therefore, they can be very useful to estimate the actual extent of lignin acylation. The main advantage of spectroscopic techniques over degradation methods is the analysis of the whole lignin structure and direct determination of the different lignin moieties and interunit linkages. In this paper, we study the structure of some naturally extensively acylated lignins occurring in several herbaceous plants (namely, sisal, kenaf, abaca, and curaua) by a combination of chemical degradative (DFRC) and spectroscopic (2D-NMR) techniques.

MATERIALS AND METHODS

Samples. The plant samples selected for this study consist of bast fibers obtained from the stalk phloem layer of kenaf (*Hibiscus cannabinus*) and leaf fibers of sisal (*Agave sisalana*), abaca (*Musa textilis*), and curaua (*Ananas erectifolius*). The fibers were finely ground to sawdust using a knife mill (Analysenmühle A10, Janke and Kunkel GmbH, Staufen, Germany) before analysis. Milled-wood lignin (MWL) was extracted from finely ball-milled (150 h) plant material, free of extractives and hot water soluble material, using dioxane/water (9:1, v/v), followed by evaporation of the solvent, and purified as described (*25*). The final yields ranged from 5 to 15% of the original lignin content. Extension of milling time, which would increase yield, was avoided to prevent chemical modifications on the lignin structure.

DFRC (Derivatization Followed by Reductive Cleavage). The DFRC degradation was performed according to the developed protocol (*26*−*28*). Lignins (10 mg) were stirred for 2 h at 50 °C with acetyl bromide in acetic acid (8:92). The solvents and excess of bromide were removed by rotary evaporation. The products were then dissolved in dioxane/acetic acid/water (5:4:1, v/v/v), and 50 mg of powered Zn was added. After 40 min of stirring at room temperature, the mixture was transferred into a separatory funnel with dichloromethane and saturated ammonium chloride. The pH of the aqueous phase was adjusted to <3 by adding 3% HCl, the mixture vigorously mixed, and the organic layer separated. The water phase was extracted twice more with dichloromethane. The combined dichloromethane fractions were dried over anhydrous $NaSO_4$, and the filtrate was evaporated in a rotary evaporator. The residue was acetylated for 1 h in 1.1 mL of dichloromethane containing 0.2 mL of acetic anhydride and 0.2 mL of pyridine. The acetylated lignin degradation products were collected after rotary evaporation of the solvents and subsequently analyzed by GC/MS. To assess the presence of naturally acetylated lignin units, a modification of the standard DFRC method by using propionylating instead of acetylating reagents (DFRC′) was used in the present study (*13, 16*).

The GC/MS analyses were performed with a Varian model Star 3800 GC equipped with an ion trap detector (Varian model Saturn 4000) using a medium-length (15 m) capillary column (DB-5HT, 5 m × 0.25 mm i.d., 0.1 *μ*m film thickness) from J&W Scientific. The oven was heated from 120 (1 min) to 330 at 6 °C/min and held for 4 min at the final temperature. The injector was programmed from 60 to 350 °C at

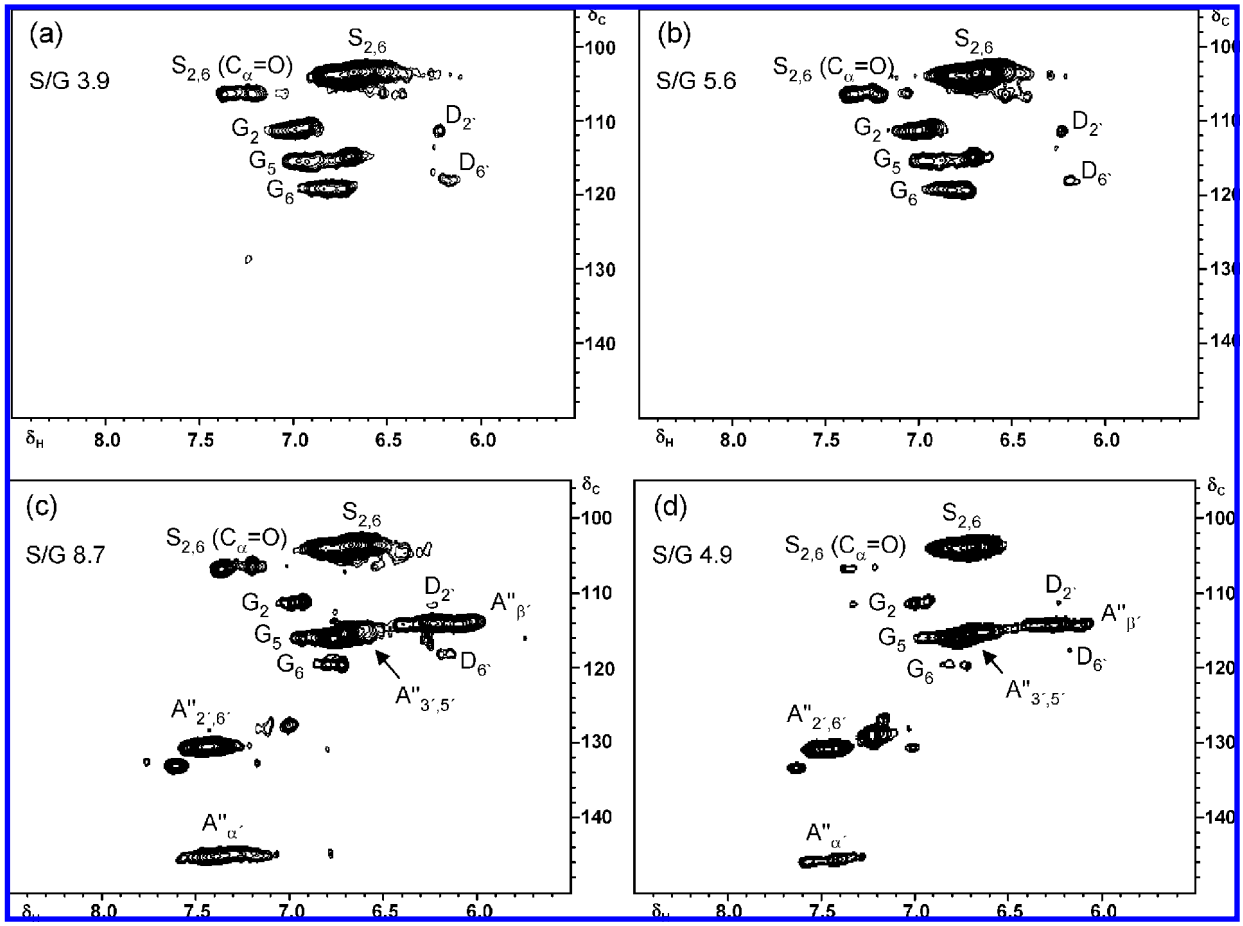

Figure 2. Expanded aromatic region, δ_C/δ_H 95−150/5.5−8.5, of the HSQC spectra of the lignins from (**a**) sisal, (**b**) kenaf, (**c**) abaca, and (**d**) curaua. See **Table 1** for signal assignment. G and S are the guaiacyl and syringyl aromatic units, respectively, A corresponds to acylating *p*-coumarate moieties, and D to spirodienone rings.

a rate of 200 °C/min and held until the end of the analysis. The transfer line was kept at 300 °C. Helium was used as the carrier gas at a rate of 2 mL/min. Quantification of the released individual monomers was performed using tetracosane as external standard and by assuming similar response factors as those of the acetylated monomers previously reported (*26*), although without authentication on our instrument. Molar yields were calculated on the basis of molecular weights of the respective acetylated and/or propionylated compounds.

NMR Spectroscopy. NMR spectra were recorded at 25 °C on a Bruker AVANCE 500 MHz equipped with a *z*-gradient triple-resonance probe. Around 40 mg of lignin was dissolved in 0.75 mL of deuterated dimethyl sulfoxide (DMSO-d_6), and 2D-NMR spectra were recorded in HSQC (heteronuclear single quantum correlation) experiments. The spectral widths were 5000 and 25000 Hz for the ^{1}H and ^{13}C dimensions, respectively. The number of collected complex points was 2048 for the ^{1}H dimension with a recycle delay of 5 s. The number of transients was 64, and 256 time increments were always recorded in the ^{13}C dimension. The $^1J_{CH}$ used was 140 Hz. The *J*-coupling evolution delay was set to 3.2 ms. Squared cosine-bell apodization function was applied in both dimensions. Prior to Fourier transform the data matrices were zero filled to 1024 points in the ^{13}C dimension. The central solvent peak was used as an internal reference (δ_C 40.1; δ_H 2.50). HSQC cross-signals were assigned by combining the results of the different experiments and comparison with the literature (*20*−*23, 29*−*32*). A semiquantitative analysis of the intensities of the HSQC cross-signal intensities was performed (*29, 33*). Because the cross-signal intensity depends on the particular $^1J_{CH}$ value, as well on the T_2 relaxation time, a direct analysis of the intensities is impossible. A more accurate quantification of the 2D HSQC NMR data analysis can be achieved by using the recently published method (*34*). Thus, the integration on the cross-signals was performed separately for the different regions of the HSQC spectra, which contain signals that correspond to chemically analogous carbon−proton pairs. For these signals, the $^1J_{CH}$ coupling value is relatively similar, their chemical shifts are also similar to each other; hence, the error of off-resonance effect is small and, therefore, can be used semiquantitatively to estimate the relative abundance of the different species. In the aliphatic oxygenated region, interunit linkages were estimated from $C_\alpha-H_\alpha$ correlations to avoid possible interference from homonuclear $^1H-^1H$ couplings, and the relative abundances of side chains involved in interunit linkages were calculated. In the aromatic region, $C_{2,6}-H_{2,6}$ correlations from S units and C_2-H_2 plus C_6-H_6 correlations from G units were used to estimate the S/G ratio of lignin, and *p*-coumaric acid content was estimated from its $C_{2,6}-H_{2,6}$ correlation signal. Lignin acylation was estimated from the intensities of $C_\gamma-H_\gamma$ correlations in acylated and nonacylated side chains.

RESULTS AND DISCUSSION

MWL is a lignin preparation considered to be the most representative of the whole native lignin in the plant (*25*), despite its low yield and the possibility of some modifications during milling (*35*). Therefore, in this work, the MWL isolated from the selected herbaceous plants (sisal, kenaf, abaca, and curaua) were analyzed by 2D-NMR and DFRC to get insight into their structural characteristics. However, we must still keep in mind that the results obtained here reflect the structure of isolated MWL, which represents only a part of the whole lignin in the plant.

HSQC-NMR Spectra of Highly Acetylated Lignins. The HSQC NMR spectra of the different MWL showed three regions corresponding to aliphatic, side-chain, and aromatic $^{13}C-^1H$ correlations. The aliphatic (nonoxygenated) region showed

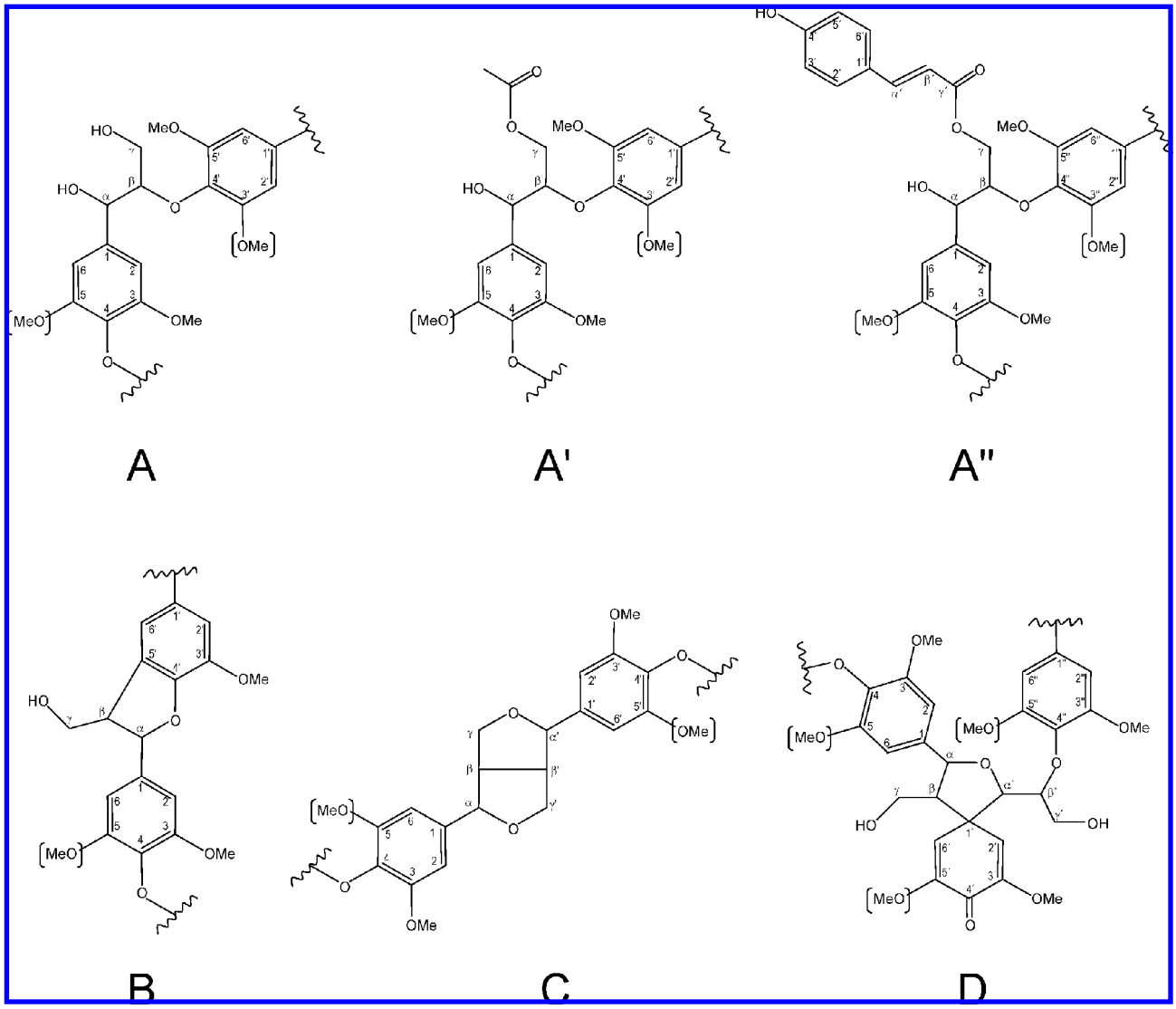

Figure 3. Main structures present in the highly acylated lignins studied here: (**A**) β-*O*-4′ linked substructures; (A′) β-*O*-4′ linked substructures with acetylated γ-carbon; (**A″**) β-*O*-4′ linked substructures; with *p*-coumaroylated γ-carbon; (**B**) phenylcoumaran structures formed by β-5′ and α-*O*-4′ linkages; (**C**) resinol structures formed by β-β′, α-*O*-γ′, and γ-*O*-α′ linkages; and (**D**) spirodienone structures formed by β-1′, and α-O-α′ linkages.

signals with no structural information (except for the presence of acetate signals at δ_C/δ_H 20.7/1.74) and therefore is not discussed in detail. The side-chain regions (δ_C/δ_H 50−90/2.5−5.5) and the aromatic regions (δ_C/δ_H 95−150/5.5−8.5) of the MWL selected for this study are shown in **Figures 1** and **2**, respectively, and the main substructures found in these lignins are depicted in **Figure 3**. The main lignin cross-signals assigned in the HSQC spectra are listed in **Table 1**.

In the side-chain region, cross-signals of methoxyls (δ_C/δ_H 56.2/3.73) and side-chains in β-*O*-4′ substructures were the most prominent in all lignins. Interestingly, the HSQC spectra clearly show the presence of intense signals corresponding to acylated γ-carbon in the range from δ_C/δ_H 63.5/3.83 to 4.30 in all lignin samples, together with the presence of signals from normal hydroxylated γ-carbon (at δ_C/δ_H 60.2/3.30 and 3.70). The spectra indicate that these lignins are extensively acylated and that acylation occurs exclusively at the γ-position of the lignin side chain. HSQC can not identify the nature of the ester, although it was shown in previous studies that acetates (and *p*-coumarates) occurred in these lignins (*12, 13, 15, 16, 36*). Traces (<0.5% of acylated γ-carbon) of a signal at δ_C/δ_H 5.87/74.66 corresponding to acylated α-carbon were found in the HSQC of sisal and kenaf MWL, although it was absent in the rest of the lignins studied here. This signal could be due to a migration of the acetyl group from the γ-carbon to the α-carbon in the lignin side-chain, as already advanced by Ralph (*12*).

An estimation of the percentage of γ-acylation of the lignin side-chain was calculated from the HSQC spectra by integration of the signals corresponding to the hydroxylated and acylated γ-carbon (**Table 2**) and ranged from 58% in kenaf bast lignin to 80% in abaca lignin. Although kenaf lignin has already been known for a long time to be highly acetylated (*12*), to our knowledge, this is the first time that this type of highly acylated lignin has been described in other plants. The high extent of lignin acylation observed in different herbaceous plants (including both mono- and eudicotyledoneous) indicates that this type of lignin might be more frequent than previously thought. Naturally acetylated lignins may also occur in many other plants, but their occurrence has probably been biased due to the limitations of the analytical procedures used for their isolation and/or structural characterization. Natural acetates present on lignin might have been hydrolyzed and removed when using traditional isolation methods (such as alkaline extraction often applied to nonwood lignins) and degradative procedures for chemical characterization (such as nitrobenzene oxidation, CuO oxidation, or thioacidolysis). Indeed, for spectroscopic analysis,

Table 1. Assignment of Main Lignin $^{13}C-^{1}H$ Cross-Signals in the MWL HSQC Spectra Shown in **Figures 1** and **2**

δ_C/δ_H	assignment
53.7/3.12	$C_\beta-H_\beta$ in β-β' (resinol) substructures (C)
56.1/3.09	$C_\beta-H_\beta$ in β-1′ (spirodienone) substructures (D)
60.0/3.38−3.71	$C_\gamma H_\gamma$ in β-*O*-4′ substructures (A)
63.8/3.83−4.30	$C_\gamma H_\gamma$ in γ-acylated β-*O*-4′ substructures (A′ and A″)
71.7/3.81 and 4.17	$C_\gamma-H_\gamma$ in β-β' (resinol) substructures (C)
72.3/4.86	$C_\alpha-H_\alpha$ in β-*O*-4′ substructures (A, A′, and A″)
82.1/5.12	$C_\alpha-H_\alpha$ in β-1′ (spirodienone) substructures (D)
83.6/4.32	$C_\beta-H_\beta$ in γ-acylated β-*O*-4′ substructures (A′ and A″)
85.4/4.64	$C_\alpha-H_\alpha$ in β-β' (resinol) substructures (C)
85.4/4.80	$C_{\alpha'}-H_{\alpha'}$ in β-1′ (spirodienone) substructures (D)
86.5/4.10	$C_\beta-H_\beta$ in γ-OH β-*O*-4′ substructures (A)
87.7/5.45	$C_\alpha-H_\alpha$ in β-5′ (phenylcoumaran) substructures (B)
103.8/6.68	C_2-H_2 and C_6-H_6 in syringyl units
106.7/7.36 and 7.21	C_2-H_2 and C_6-H_6 in oxidized (C_α=O) syringyl units
111.5/6.99	C_2-H_2 in guaiacyl units
111.6/6.23	$C_{2'}-H_{2'}$ in β-1′ (spirodienone) substructures (D)
114.3/6.24	$C_{\beta'}-H_{\beta'}$ in *p*-coumaroylated substructures (A″)
115.2/6.71 and 6.94	C_5-H_5 in guaiacyl units
116.2/6.77	$C_{3'}-H_{3'}$ and $C_{5'}-H_{5'}$ in *p*-coumaroylated substructures (A″)
118.3/6.19	$C_{6'}-H_{6'}$ in β-1 (spirodienone) substructures (D)
119.5/6.83	C_6-H_6 in guaiacyl units
130.5/7.4	$C_{2'}-H_{2'}$ and $C_{6'}$-$H_{6'}$ in *p*-coumaroylated substructures (A″)
145.1/7.39	$C_{\alpha'}-H_{\alpha'}$ in *p*-coumaroylated substructures (A″)

Table 2. Structural Characteristics (Percentage of γ-Acylation, Relative Abundance of the Main Interunit Linkages as Percentages of Side-Chains Involved, and S/G Ratio) Observed from the HSQC Spectra of the Selected MWL

	sisal	kenaf	abaca	curaua
percentage of γ-acylation	68	58	80	69
β-*O*-4′ alkyl-aryl ether	89	84	94	94
β-1′ (spirodienone)	5	6	6	4
β-5′ (phenylcoumaran)	2	2	0	2
β-β' (syringaresinol)	4	8	0	0
S/G ratio	3.9	5.6	8.7	4.9

for example, using NMR, lignin is frequently in vitro acetylated for improved solubility and spectroscopic properties, which prevented the detection of natural lignin acetylation.

The side-chain region of the HSQC spectra gives also additional information about the interunit linkages present in the structure of these lignins. All of the spectra showed prominent signals corresponding to β-*O*-4′ aryl ether linkages. The $C_\alpha-H_\alpha$ correlations in β-*O*-4′ substructures were observed at δ_C/δ_H 72.3/4.86 (structures A, A′, and A″), whereas the $C_\beta-H_\beta$ correlations were observed at δ_C/δ_H 86.5/4.10 in normal γ-hydroxylated β-*O*-4′ aryl ether substructures (A) but shifted to δ_C/δ_H 83.6/4.32 in γ-acylated β-*O*-4′ aryl ether substructures (A′ and A″). β-*O*-4′ aryl ether substructures were highly predominant in all of the lignins analyzed here, although other substructures were also observed. Small signals corresponding to spirodienone (β-1′ and α-*O*-α′ linkages) substructures (D) can be observed in the spectra of sisal, kenaf, abaca, and curaua lignins. Signals of spirodienone $C_\alpha-H_\alpha$, $C_{\alpha'}-H_{\alpha'}$, and $C_\beta-H_\beta$ correlations were observed at δ_C/δ_H 85.4/4.64, 85.4/4.80 and 56.1/3.09, respectively. Spirodienone substructures were previously reported in the lignin from kenaf bast fibers by Zhang et al. (*37*). Phenylcoumaran (β-5′ linkages) substructures (B) were also found, although in very small proportions. Very weak signals corresponding to $C_\alpha-H_\alpha$ correlations of phenylcoumaran

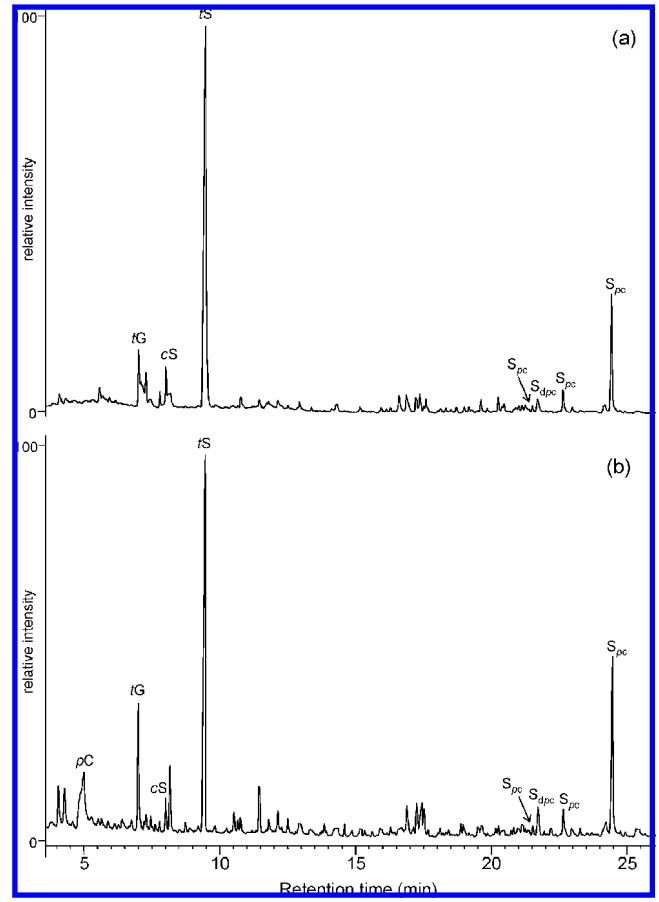

Figure 4. Chromatograms of the DFRC degradation products of the MWL from (**a**) abaca and (**b**) curaua, showing the presence of sinapyl alcohol esterified to *p*-coumarate moieties. S_{dpc} and S_{pc} are the sinapyl alcohol esterified with dihydro-*p*-coumarate and *p*-coumarate, respectively (as their acetyl derivative). *c*G, *t*G, *c*S, and *t*S are the normal *cis*- and *trans*-guaiacyl and syringyl monomers, respectively (as their acetyl derivatives).

Table 3. Abundance (Molar Yields) of the DFRC and DFRC′ Degradation Monomers of the MWL Isolated from the Different Plants Selected for This Study and Relative Abundances of the Different Acylated (Acetylated and *p*-Coumaroylated) Lignin Moieties

	monomers (μmol/g of lignin)										
	G	G_{ac}	G_{pc}	S	S_{ac}	S_{pc}	$\%S_{ac}$[a]	$\%S_{pc}$[b]	$\%G_{ac}$[c]	$\%G_{pc}$[d]	S/G
sisal	122	124	0	108	378	0	78	0	50	0	2.0
kenaf	390	38	0	543	780	0	59	0	9	0	3.1
abaca	50	3	1	21	131	124	48	45	6	2	5.1
curaua	250	252	3	515	595	195	46	15	50	1	2.6

[a] $\%S_{ac}$ is the percentage of acetylated S units with respect to the total S units. [b] $\%S_{pc}$ is the percentage of *p*-coumaroylated S units with respect to the total S units. [c] $\%G_{ac}$ is the percentage of acetylated G units with respect to the total G units. [d] $\%G_{pc}$ is the percentage of *p*-coumaroylated G units with respect to the total G units.

substructures at δ_C/δ_H 87.7/5.45 were observed in the spectra of sisal, kenaf, and curaua lignins, but were absent in the spectrum of abaca. The presence of these low amounts of phenylcoumaran substructures was expected due to the very low levels of guaiacyl lignin units in all of these samples. Finally, resinol (β-β' linkages) substructures (C) were clearly observed in the spectrum of kenaf. Signals for the $C_\alpha-H_\alpha$ and $C_\beta-H_\beta$ and the double $C_\gamma-H_\gamma$ correlations of resinol substructures were observed at δ_C/δ_H 85.4/4.64, 53.7/3.12 and 71.7/3.81 and 4.17, respectively. Resinol substructures could also be observed, although in small traces, in the spectrum of sisal, but were

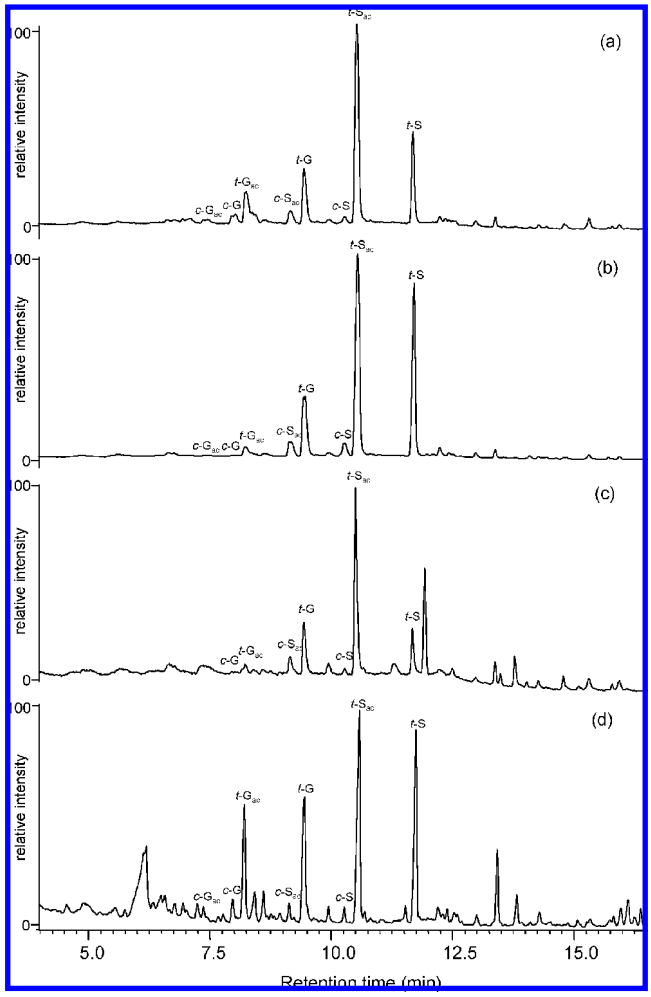

Figure 5. Chromatograms of the DFRC′ degradation products of MWL from (**a**) sisal, (**b**) kenaf, (**c**) abaca, and (**d**) curaua. *c*-G, *t*-G, *c*-S, and *t*-S are the normal *cis*- and *trans*-guaiacyl and -syringyl monomers, respectively (as their propionylated derivatives). *c*-G_{ac}, *t*-G_{ac}, *c*-S_{ac}, and *t*-S_{ac} are the originally acetylated *cis*- and *trans*-guaiacyl and -syringyl monomers, respectively (as their propionylated derivatives).

completely absent in the spectra of abaca and curaua lignins. The relative abundances of the main interunit linkages present in the MWL selected for this study were calculated from the HSQC spectra and are shown in **Table 2**. All of these highly acetylated lignins share a common characteristic, the strikingly high proportion of *β-O-4′* ether linkages (up to 94% of all linkages) and a very low proportion of carbon-carbon linkages (i.e., *β-1′*, *β-5′*, and *β-β′*). Some of these linkages (*β-5′* and *β-β′*) are even absent in some lignins (abaca and curaua).

The main cross-signals in the aromatic region of the HSQC spectra (**Figure 2**) correspond to the aromatic rings of the different lignin units. Signals from syringyl (S) and guaiacyl (G) lignin units can be observed in all spectra. The syringyl units show a prominent signal for the $C_{2,6}-H_{2,6}$ correlation at δ_C/δ_H 103.8/6.68, whereas guaiacyl units showed different correlations for C_2-H_2 (δ_C/δ_H 111.5/6.99), C_5-H_5 (δ_C/δ_H 115.2/6.71 and 6.94), and C_6-H_6 (δ_C/δ_H 119.5/6.83). Signals corresponding to $C_{2,6}-H_{2,6}$ correlations in Cα-oxidized S-lignin units were observed at δ_C/δ_H 106.7/7.36 and 7.21. No signals for *p*-hydroxyphenyl (H) lignin units could be detected in the HSQC spectra of these lignins. An estimation of the relative proportions of the S- and G-lignin units in the HSQC spectra revealed that all of the lignins selected for this study present a very high S/G ratio, ranging from 3.9 in sisal to 8.7 in abaca (**Table 2**). Other signals present in this region of the HSQC spectra are from spirodienone substructures (D) with $C_{2'}-H_{2'}$ and $C_{6'}-H_{6'}$ correlations at δ_C/δ_H 111.6/6.23 and 118.3/6.19, respectively. Prominent signals corresponding to *p*-coumarate structures were observed in the lignins of abaca and curaua. Cross-signals corresponding to the correlations $C_{2',6'}-H_{2',6'}$ at δ_C/δ_H 130.5/7.40 and $C_{3',5'}-H_{3',5'}$ at δ_C/δ_H 116.2/6.77 of the aromatic ring and signals for the correlations of the unsaturated $C_{\alpha'}-H_{\alpha'}$ at δ_C/δ_H 145.1/7.39 and $C_{\beta'}-H_{\beta'}$ at 114.3/6.24 of the *p*-coumarate unit in structure A″ of **Figure 3** were observed in this region of the HSQC spectra of abaca and curaua. In abaca lignin, *p*-coumaric acid has already been reported to be esterified to the lignin polymer (*8, 16, 35, 38*).

Degradation Followed by Reductive Cleavage (DFRC and DFRC′). The HSQC data shown above indicate that these lignins are extensively acylated at the *γ*-position of the side chain, but cannot provide additional information on the nature of the acyl group (besides the occurrence of acetate and *p*-coumarate moieties). A sensitive and selective method is therefore needed to reveal the nature of the acyl group that is esterifying the *γ*-carbon of the lignin side chain and to know to which lignin moiety it is attached. The DFRC degradation method, which cleaves α- and *β*-ether linkages in the lignin polymer leaving *γ*-esters intact (*26*−*28*), seems to be the most appropriate method for the analysis of native *γ*-acylated lignin.

DFRC analysis of the lignin samples selected for this study allowed confirmation that *p*-coumarate groups are attached to the *γ*-carbon of abaca and curaua lignins and predominantly on syringyl units (**Figure 4**). Saturated side-chain *p*-coumarate (dihydro-*p*-coumarate) esterified to sinapyl alcohol (as its acetate derivative, S_{dpc}) was expected to be the major DFRC degradative compound, according to Lu and Ralph (*9*), and this was the only degradation product that was quantified in our previous paper (*16*). However, a closer look at other major degradation compounds produced upon DFRC of abaca and curaua lignins indicated the release of important amounts of the unsaturated side-chain counterpart, that is, intact sinapyl *p*-coumarate (as its acetate derivative, S_{pc}), that was biased, and therefore not quantified, in our previous paper. Therefore, in this work, we have now taken into account both compounds to quantify the total abundance of sinapyl *p*-coumarate units present in these lignins (**Table 3**). Trace amounts of the respective coniferyl *p*-coumarate could also de detected in abaca and curaua lignins. Moreover, some amounts of free *p*-coumaric acid (as its acetate derivative) could be observed among the DFRC degradation products of curaua lignin as a broad peak (**Figure 4**), which could probably correspond to *p*-coumaric acid moieties linked to lignin through *β-O-4′* aryl-ether bonds.

The original DFRC degradation method, however, does not allow the analysis of native acetylated lignin because the degradation products are acetylated during the degradation procedure, but with appropriate modification of the protocol by substituting acetylating reagents with propionylating reagents, DFRC′, it is also possible to obtain information about the occurrence of native lignin acetylation (*13*). **Figure 5** shows the chromatograms of the DFRC′ products released from the lignin samples selected in this study. All of the analyzed lignins released the *cis* and *trans* isomers of guaiacyl (*c*-G and *t*-G) and syringyl (*c*-S and *t*-S) lignin monomers (as their propionylated derivatives) arising from normal *γ*-OH units in lignin. In addition, the presence of originally *γ*-acetylated guaiacyl (*c*-G_{ac} and *t*-G_{ac}) and syringyl (*c*-S_{ac} and *t*-S_{ac}) lignin units could also be clearly observed in the chromatograms of all of the selected lignins indicating that acetylation occurred exclusively

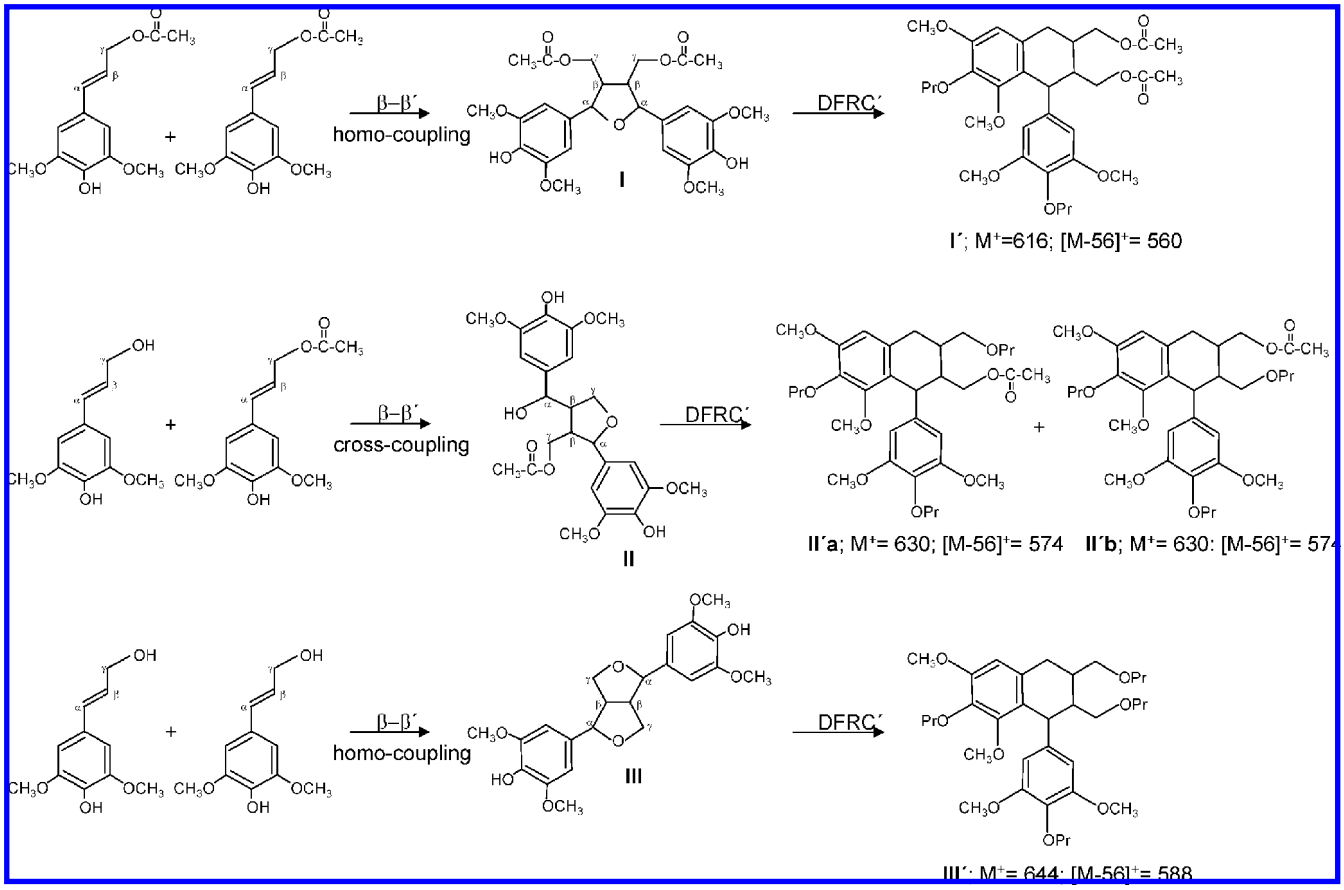

Figure 6. Structures of the tetrahydrofuran dimers arising from the β-β' coupling of sinapyl alcohol and sinapyl acetate: (**I**) β-β' coupling product of two sinapyl acetates; (**II**) β-β' coupling product of a sinapyl alcohol and a sinapyl acetate; (**III**) β-β' coupling product (syringaresinol) of two sinapyl alcohols. The aryltetralin products expected from the DFRC′ degradation of these tetrahydrofuran moieties are also shown, with indication of their molecular weight and base peak in their mass spectra. Adapted from Lu and Ralph (*14*).

at the γ-carbon of the lignin side chain, as already observed in the HSQC spectra.

The results from the DFRC and DFRC′ analysis of the MWL selected for this study, namely, the molar yields of the released monomers, the percentages of naturally acetylated guaiacyl (%G_{ac}) and syringyl (%S_{ac}) and *p*-coumaroylated guaiacyl (%G_{pc}) and syringyl (%S_{pc}) lignin moieties, and the S/G ratios are presented in **Table 3**. The data indicate that a high extent of γ-acetylation occurs in all lignins studied here and that *p*-coumaric acid is also found partially esterifying the lignin of abaca and curaua, in agreement with the NMR data. In all cases, acetate and *p*-coumarate groups are preferentially attached to syringyl units, as previously noted for other lignins (*7*−*9, 12*−*16, 39*). Interestingly, the high extent of acetylation observed in sisal and curaua also included the G-lignin units (around 50% of acetylation in both cases). By contrast, in kenaf and abaca lignins, the γ-carbon of G-lignin units is mostly not esterified. On the other hand, the high extent of acylation of the lignin monomers observed by the DFCR (and DFRC′) method, which can analyze only noncondensed lignin moieties, is in accordance with the high extent of lignin acylation observed by HSQC technique, which allows the analysis of the entire MWL structure, including both condensed and noncondensed linkages. This fact indicates that both condensed and noncondensed moieties have similar extents of acylation. However, we must now convey again that the results presented here reflect only the structure of the isolated MWL, which represents only a small part of the entire native lignin. However, similar lignin S/G ratio and acylation degree have been found by in situ analysis in HSQC spectra of the whole cell wall material (without lignin isolation) at the gel state (*40*), indicating that MWL can still be considered as the most representative preparation for the plant native lignin, despite its low yield.

Previous papers describing the structure of some of these lignins have failed to detect their high levels of acetylation. A recent paper describing the structure of sisal lignin (*41*) did not detect the high levels of acetylation, despite the use of spectroscopic techniques. Probably, this was due to the method used for isolation (acidolysis) that might have hydrolyzed the acetyl groups or a misassignment of the spectral bands. Previous structural studies on abaca lignin (*8, 16, 36, 38*), using different degradation methods, also suggested the occurrence of *p*-coumaroylated units attached to the γ-carbon of the lignin side chain. The presence of acetylated γ-carbons was also observed in abaca fibers directly by Py-GC/MS (*15*), although other authors failed to detect their presence (*8*).

On the other hand, the question as to whether acylated lignin derives from polymerization of acylated monolignols or from acylation of the lignin polymer has recently been addressed, and sinapyl acetate has been demonstrated to behave as a monomer in lignification participating in coupling reactions (*14, 16, 17, 42*). Part of the evidence comes from the β-β' coupling reactions. If the γ-carbon of a monolignol is preacylated, the formation of the normal β-β' resinol structures cannot occur because the absence of free γ-hydroxyls needed to rearomatize the quinone methide moiety. Instead, new tetrahydrofuran structures are formed from the β-β' homo- and cross-coupling of two sinapyl (acylated and nonacylated) monolignols, as advanced by Lu and Ralph (*14*) (**Figure 6**). It is clear that tetrahydrofuran structures I and II can be formed only if sinapyl

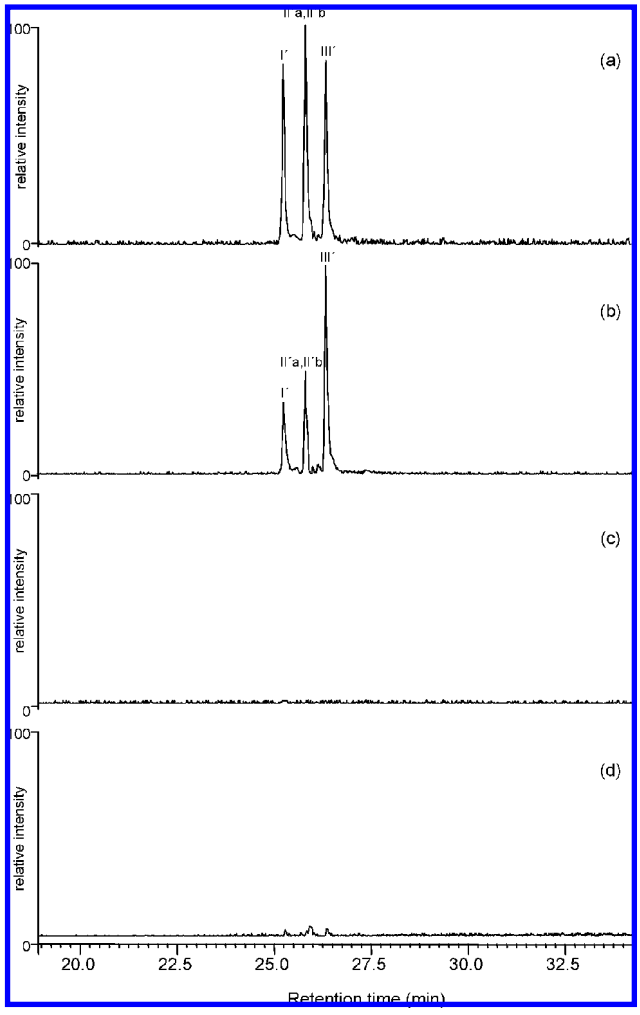

Figure 7. Detail of reconstructed chromatogram (sum of the characteristic ions at *m*/*z* 560, 574, and 580) of the DFRC′ degradation products of the MWL from (**a**) sisal, (**b**) kenaf, (**c**) abaca, and (**d**) curaua, showing the presence of aryltetralin *β*-*β*′ products containing two (**I′**), one (**II′a** and **II′b**), and no (**III′**) native acetates.

alcohol is preacetylated (at monomer stage) and then undergoes *β*-*β*′ coupling. Therefore, the presence of these tetrahydrofuran substructures in the lignin polymer would be indicative of the occurrence of preacylated monolignols. In this work, we have investigated the presence of the tetrahydrofuran structures arising from *β*-*β*′ coupling of sinapyl acetate in the MWL selected for this study by DFRC′. The expected DFRC′ degradation products of the tetrahydrofuran *β*-*β*′ structures, as suggested by Lu and Ralph (*14*), are also indicated in **Figure 6**. **Figure 7** shows the reconstructed chromatograms (sum of the single ion chromatograms of the respective base peaks) of the DFRC′ degradation products of the expected tetrahydrofuran dimers arising from the *β*-*β*′ coupling of the sinapyl monolignols. Interestingly, compounds derived from the DFRC′ of homocoupling (**I′**) and cross-coupling (**II′a** and **II′b**) of sinapyl acetate were clearly observed in the lignins of sisal and kenaf, clearly indicating that in these lignins sinapyl alcohol is preacetylated and behaves as a real monolignol participating in postcoupling reactions. However, in the case of abaca and curaua lignins, no traces of any type of *β*-*β*′ linkage (including syringaresinol and the new tetrahydrofuran structures) could be detected after DFRC, in agreement with the absence of these linkages observed in the HSQC spectra.

The presence of cross-coupling structures of sinapyl alcohol and sinapyl acetate indicates that both monolignols are produced simultaneously by the plant. Moreover, the relative abundance of the compounds released in **Figure 7** gives some additional information. In sisal, the relative molar abundance of the acetylated versus the nonacetylated sinapyl alcohols forming *β*-*β*′ linkages (taking into account that dimer **I′** consists of two sinapyl acetates, dimers **II′** consist of one sinapyl acetate and one sinapyl alcohol, and dimer **III′** consists of two sinapyl alcohols) is 44:56, with a slight predominance of the nonacetylated sinapyl alcohol, whereas their relative molar abundance in ether-linked structures is 78:22, with a strong predominance of sinapyl acetate. A similar trend is also observed in kenaf lignin, where the relative molar abundance of the acetylated versus the nonacetylated sinapyl alcohols forming *β*-*β*′ linkages is 23:77, with a predominance of the nonacetylated sinapyl alcohol, whereas their relative molar abundances in ether-linked structures is 59:41, with a strong predominance of sinapyl acetate. This indicates that sinapyl acetate has a lower tendency to form *β*-*β*′ linkages than the normal sinapyl alcohol, and therefore those lignins having a high extent of acetylation would produce lower amounts of *β*-*β*′ linkages, as already advanced (*16*). This means that, probably, the high level of lignin acetylation is related in some way with the low presence of *β*-*β*′ linkages. This is in agreement with the high proportions of *β*-*O*-4′ aryl ether substructures and the low proportion of *β*-*β*′ substructures present in these lignins, as observed in the HSQC spectra shown above. Therefore, it seems that the high extent of *γ*-acetylation would favor the formation of a predominantly *β*-*O*-4 lignin structure, which is indeed devoid of *β*-*β*′ linkages.

It has been reported that in vitro peroxidase−H_2O_2 oxidation of equimolar amounts of sinapyl alcohol and *γ*-acylated sinapyl alcohol produced equal amounts of the expected *β*-*β*′ coupled and cross-coupled products (**I**, **II**, and **III**) shown in **Figure 6**, in a ratio 1:2:1, suggesting that the coupling reactions were insensitive to the acylation of the *γ*-carbon (*17, 18*). However, this is not the case of what we have seen that occur in the plants, where sinapyl acetate seems to have a lower tendency to form *β*-*β*′ linkages and, therefore, a high abundance of acetylated lignin monomers will ultimately produce a lignin with very low levels of *β*-*β*′ structures during lignification. Therefore, a discrepancy exists between what is observed in vitro and in the plant. Moreover, as indicated by Lu and Ralph (*17*), from the two possible stereoisomers of the *β*-*β*′ homodimerization product of sinapyl acetate (structure **I** in **Figure 6**), the isomer produced during in vitro coupling reactions is not the same as that present in plants. Whether there is a protein (or any other mechanism) in the plant controlling the *β*-*β*′ coupling reaction needs additional investigations.

Structural Features of Highly Acylated Lignins. The lignins selected for this study share some common structural features. First, they are characterized for being extensively acylated (with either acetate or *p*-coumarate groups), exclusively at the *γ*-carbon of the lignin side chain and preferentially over syringyl units. Moreover, all of these lignins present a high predominance of syringyl over guaiacyl lignin units, and a very high predominance of *β*-*O*-4′ linkages, (with a very low proportion of *β*-*β*′, *β*-5′ and other linkages) that make these lignins very linear and unbranched. In particular, sisal and kenaf lignins present a high extent of *γ*-acylation, exclusively with acetate groups and preferentially on S-lignin moieties in the case of kenaf lignin and over both S- and G-lignin moieties in the case of sisal lignin. In both cases, *β*-*O*-4′ aryl ether linkages predominate, although some *β*-*β*′ (resinol) and *β*-1′ (spirodienones) linkages are observed in low proportions. On the other

hand, the structure of abaca lignin is assembled mostly with syringyl units with a high extent of acylation of the γ-carbon with both acetate and *p*-coumarate groups. β-*O*-4′ linkages are also predominant in this lignin. No β-β' linkages are present, but some β-1′ (spirodienones) linkages can be observed in abaca lignin. Finally, the lignin of curaua has a predominance of S-lignin units, a predominance of β-*O*-4′ linkages, and a high extent of acylation at the γ-carbon with acetate and *p*-coumarate groups, acetate groups being also esterifying to a high extent the γ-carbon of G-lignin units. In general, all of these structural features make these lignins very different from the structural models already proposed for softwood (*43, 44*) and hardwood (*45*) lignins. All subsequent lignin structural studies, including those in plant genetics or plant breeding projects, should take into account the occurrence of lignin acylation, which in many plants takes place at very high levels, as seen above, and which have often been overlooked in the past; otherwise, the conclusions drawn may not be representative of the real native lignin structure.

Conclusions. The structure of the MWL isolated from the herbaceous plants sisal, kenaf, abaca, and curaua has been elucidated by 2D-NMR and DFRC techniques. The analyses indicated that the lignins from these plants are extensively acylated at the γ-carbon of the lignin side chain (with either acetate and/or *p*-coumarate groups) and preferentially on syringyl moieties. The structure of these highly acetylated lignins can be essentially regarded as syringyl units linked mostly through β-*O*-4′ ether bonds, where the γ-carbons of the side chains are extensively acylated. The lignin polymer is therefore extremely linear and unbranched. The study of highly acylated lignins will significantly contribute to the redefinition of the structure of lignin and complete the lignin biosynthetic pathway.

LITERATURE CITED

(1) Sarkanen, K. V.; Ludwig, C. H. Definition and nomenclature. In *Lignins: Occurrence, Formation, Structure, and Reactions*; Sarkanen, K. V.; Ludwig, C. H., Eds.; Wiley-Interscience: New York, 1971; pp 1−16.

(2) Boerjan, W.; Ralph, J.; Baucher, M. Lignin biosynthesis. *Annu. Rev. Plant Biol.* **2003**, *54*, 519–546.

(3) Ralph, J.; Lundquist, K.; Brunow, G.; Lu, F.; Kim, H.; Schatz, P. F.; Marita, J. M.; Hatfield, R. D.; Ralph, S. A.; Christensen, J. H.; Boerjan, W. Lignins: natural polymers from oxidative coupling of 4-hydroxyphenylpropanoids. *Phytochem. Rev.* **2004**, *3*, 29–60.

(4) Smith, D. C. C. *p*-Hydroxybenzoate groups in the lignin of aspen (*Populus tremula*). *J. Chem. Soc.* **1955**, 2347–2351.

(5) Nakano, J.; Ishizu, A.; Migata, N. Studies on lignin. XXXII. Ester groups of lignin. *Tappi* **1961**, *44*, 30–32.

(6) Landucci, L. L.; Deka, G. C.; Roy, D. N. A. ^{13}C NMR study of milled wood lignins from hybrid *Salix* clones. *Holzforschung* **1992**, *46*, 505–511.

(7) Ralph, J.; Hatfield, R. D.; Quideau, S.; Helm, R. F.; Grabber, J. H.; Jung, H.-J. G. Pathway of *p*-coumaric acid incorporation into maize lignin as revealed by NMR. *J. Am. Chem. Soc.* **1994**, *116*, 9448–9456.

(8) Sun, R. C.; Fang, J. M.; Goodwin, A.; Lawther, J. M.; Bolton, J. Fractionation and characterization of ball-milled and enzyme lignins from abaca fibre. *J. Sci. Food Agric.* **1999**, *79*, 1091–1098.

(9) Lu, F.; Ralph, J. Detection and determination of *p*-coumaraloylated units in lignin. *J. Agric. Food Chem.* **1999**, *47*, 1985–1992.

(10) Meyermans, H.; Morreel, K.; Lapierre, C.; Pollet, B.; De Bruyn, A.; Busson, R.; Herdewijn, P.; Devreese, B.; Van Beeumen, J.; Marita, J. M.; Ralph, J.; Chen, C.; Burggraeve, B.; Van Montagu, M.; Messens, E.; Boerjan, W. Modification in lignin and accumulation of phenolic glucosides in poplar xylem upon down-regulation of caffeoyl-coenzyme A *O*-methyltransferase, an enzyme involved in lignin biosynthesis. *J. Biol. Chem.* **2000**, *275*, 36899–36909.

(11) Crestini, C.; Argyropoulos, D. S. Structural analysis of wheat straw lignin by quantitative ^{31}P and 2D NMR spectroscopy. The occurrence of ester bonds and α-O-4 substructures. *J. Agric. Food Chem.* **1997**, *45*, 1212–1219.

(12) Ralph, J. An unusual lignin from kenaf. *J. Nat. Prod.* **1996**, *59*, 341–342.

(13) Ralph, J.; Lu, F. The DFRC method for lignin analysis. 6. A simple modification for identifying natural acetates in lignin. *J. Agric. Food Chem.* **1998**, *46*, 4616–4619.

(14) Lu, F.; Ralph, J. Preliminary evidence for sinapyl acetate as a lignin monomer in kenaf. *Chem. Commun.* **2002**, 90–91.

(15) del Río, J. C.; Gutiérrez, A.; Martínez, A. T. Identifying acetylated lignin units in non-wood fibers using pyrolysis-gas chromatography/mass spectrometry. *Rapid Commun. Mass Spectrom.* **2004**, *18*, 1181–1185.

(16) del Río, J. C.; Marques, G.; Rencoret, J.; Martínez, A. T.; Gutiérrez, A. Occurrence of naturally acetylated lignin units. *J. Agric. Food Chem.* **2007**, *55*, 5461–5468.

(17) Lu, F.; Ralph, J. Novel β-β structures in lignins incorporating acylated monolignols. *Appita* **2005**, 233–237.

(18) Lu, F.; Ralph, J.; Morreel, K.; Messens, E.; Boerjan, W. Preparation and relevance of a cross-coupling product between sinapyl alcohol and sinapyl *p*-hydroxybenzoate. *Org. Biomol. Chem.* **2004**, 2888–2890.

(19) Morreel, K.; Ralph, J.; Kim, H.; Lu, F.; Goeminne, G.; Ralph, S. A.; Messens, E.; Boerjan, W. Profiling of oligolignols reveals monolignols coupling conditions in lignifying poplar xylem. *Plant Physiol.* **2004**, *136*, 3537–3549.

(20) Ralph, J.; Marita, J. M.; Ralph, S. A.; Hatfield, R. D.; Lu, F.; Ede, R. M.; Peng, J.; Quideau, S.; Helm, R. F.; Grabber, J. H.; Kim, H.; Jimenez-Monteon, G.; Zhang, Y.; Jung, H.-J. G.; Landucci, L. L.; MacKay, J. J.; Sederoff, R. R.; Chapple, C.; Boudet, A. M. Solution-state NMR of lignin. In *Advances in Lignocellulosics Characterization*; Argyropoulos, D. S., Ed.; Tappi Press: Atlanta, GA, 1999; pp 55−108.

(21) Ralph, S. A.; Ralph, J.; Landucci, L. NMR database of lignin and cell wall model compounds;U.S. Forest Products Laboratory, Madison, WI, 2004 (http://ars.usda.gov/Services/docs.htm?docid=10491 (accessed July 2006).

(22) Capanema, E. A.; Balakshin, M. Y.; Kadla, J. F. A comprehensive approach for quantitative lignin characterization by NMR spectroscopy. *J. Agric. Food Chem.* **2004**, *52*, 1850–1860.

(23) Capanema, E. A.; Balakshin, M. Y.; Kadla, J. F. Quantitative characterization of a hardwood milled wood lignin by nuclear magnetic resonance spectroscopy. *J. Agric. Food Chem.* **2005**, *53*, 9639–9649.

(24) Balakshin, M. Y.; Capanema, E. A.; Chen, C.-L.; Gracz, H. S. Elucidation of the structures of residual and dissolved pine kraft lignins using an HMQC NMR technique. *J. Agric. Food Chem.* **2003**, *51*, 6116–6127.

(25) Björkman, A. Studies on finely divided wood. Part I. Extraction of lignin with neutral solvents. *Sven. Papperstidn.* **1956**, *59*, 477–485.

(26) Lu, F.; Ralph, J. Derivatization followed by reductive cleavage (DFRC method), a new method for lignin analysis: protocol for analysis of DFRC monomers. *J. Agric. Food Chem.* **1997**, *45*, 2590–2592.

(27) Lu, F.; Ralph, J. The DFRC method for lignin analysis. 1. A new method for β-aryl ether cleavage: lignin model studies. *J. Agric. Food Chem.* **1997**, *45*, 4655–4660.

(28) Lu, F.; Ralph, J. The DFRC method for lignin analysis. 2. Monomers from isolated lignin. *J. Agric. Food Chem.* **1998**, *46*, 547–552.

(29) Liitiä, T. M.; Maunu, S. L.; Hortling, B.; Toikka, M.; Kilpeläinen, I. Analysis of technical lignins by two- and three-dimensional NMR spectroscopy. *J. Agric. Food Chem.* **2003**, *51*, 2136–2143.

(30) Ämmälahti, E.; Brunow, G.; Bardet, M.; Robert, D.; Kilpeläinen, I. Identification of side-chain structures in a poplar lignin using three-dimensional HMQC-HOHAHA NMR spectroscopy. *J. Agric. Food Chem.* **1998**, *46*, 5113–5117.

(31) Ibarra, D.; Chávez, M. I.; Rencoret, J.; del Río, J. C.; Gutiérrez, A.; Romero, J.; Camarero, S.; Martínez, M. J.; Jiménez-Barbero, J.; Martínez, A. T. Lignin modification during *Eucalyptus globulus* kraft pulping followed by totally chlorine free bleaching: a two dimensional nuclear magnetic resonance, Fourier transform infrared, and pyrolysis-gas chromatography/mass spectrometry study. *J. Agric. Food Chem.* **2007**, *55*, 3477–3490.

(32) Ibarra, D.; Chávez, M. I.; Rencoret, J.; del Río, J. C.; Gutiérrez, A.; Romero, J.; Camarero, S.; Martínez, M. J.; Jiménez-Barbero, J.; Martínez, A. T. Structural modification of eucalypt pulp lignin in a totally chlorine free bleaching sequence including a laccase-mediator stage. *Holzforschung* **2007**, *61*, 634–646.

(33) Heikkinen, S.; Toikka, M. M.; Karhunen, P. T.; Kilpeläinen, I. A. Quantitative 2D HSQC (Q-HSQC) via suppression of J-dependence of polarization transfer in NMR spectroscopy: application to wood lignin. *J. Am. Chem. Soc.* **2003**, *125*, 4362–4367.

(34) Zhang, L.; Gellerstedt, G. Quantitative 2D HSQC NMR determination of polymer structures by selecting the suitable internal standard references. *Magn. Reson. Chem.* **2007**, *45* (1), 37–45.

(35) Holtman, K. H.; Chang, H. M.; Jameel, H.; Kaddla, J. F. Quantitative ^{13}C NMR characterization of milled wood lignins isolated by different milling techniques. *J. Wood Chem. Technol.* **2006**, *26*, 21–34.

(36) del Río, J. C.; Gutiérrez, A.; Rodríguez, I. M.; Ibarra, D.; Martínez, A. T. Composition of non-woody plant lignins and cinnamic acids by Py-GC/MS, Py/TMAH and FT-IR. *J. Anal. Appl. Pyrolysis* **2007**, *79*, 39–46.

(37) Zhang, L.; Gellerstedt, G.; Ralph, J.; Lu, F. NMR studies on the occurrence of spirodienone structures in lignins. *J. Wood Chem. Technol.* **2006**, *26*, 65–79.

(38) del Río, J. C.; Gutiérrez, A. Chemical composition of abaca (*Musa textilis*) leaf fibers used for manufacturing of high quality paper pulps. *J. Agric. Food Chem.* **2006**, *54*, 4600–4610.

(39) Grabber, J. H.; Quideau, S.; Ralph, J. *p*-Coumaroylated syringyl units in maize lignin; implications for β-ether cleavage by thioacidolysis. *Phytochemistry* **1996**, *43*, 1189–1194.

(40) Rencoret, J.; Marques, G.; Gutiérrez, A.; Nieto, L.; Santos, J. I.; Jiménez-Barbero, J.; Martínez, A. T.; del Río, J. C. "In situ" analysis of lignin by 2D-NMR of wood (*Eucalyptus globulus* and *Picea abies*) and non-woody (*Agave sisalana*) plant materials at the gel state. *Proc. EWLP*, Stockholm, Sweden, Aug 26−29, 2008.

(41) Megiatto, J. D.; Hoareau, W.; Gardrat, C.; Frollini, E.; Castellain, A. Sisal fibers: surface chemical modification using reagent obtained from a renewable source; characterization of hemicellulose and lignin as model study. *J. Agric. Food Chem.* **2007**, *55*, 8576–8584.

(42) Ralph, J. What makes a good monolignol substitute? In *The Science and Lore of the Plant Cell Wall Biosynthesis, Structure and Function*; Hayashi, T., Ed.; Universal Publishers (Brown-Walker Press): Boca Raton, FL, 2006; pp 285−293.

(43) Adler, E. Lignin chemistry—past, present and future. *Wood Sci. Technol.* **1977**, *11*, 169–218.

(44) Brunow, G. Methods to reveal the structure of lignin. In *Lignin, Humic Substances and Coal*; Hofrichter, M.; Steinbüchel, A., Eds.; Wiley-VHC: Weinheim, Germany, 2001; Vol. 1, pp 89−116.

(45) Nimz, H. Beech lignin—proposal of a constitutional scheme. *Agnew. Chem.* **1974**, *13* (5), 313–321.

Received for review March 18, 2008. Revised manuscript received August 21, 2008. Accepted August 22, 2008. This study has been supported by the Spanish MEC (Projects AGL2005-01748 and BIO2007-28719-E) and EU Contract NMP2-CT-2006-26456 (BIORENEW). J.R. thanks the Spanish CSIC for an I3P fellowship; G.M. thanks the Spanish Ministry of Education for an FPI fellowship.

JF800806H